Diagnosing the Nature of the 125-126 GeV LHC Higgs-like signal

Jack Gunion
U.C. Davis

Orsay, March 26, 2013

Higgs couplings Collaborators: Belanger, Beranger, Ellwanger, Kraml

1. *"Status of invisible Higgs decays"* G. Belanger, B. Dumont, U. Ellwanger, J. F. Gunion and S. Kraml. arXiv:1302.5694 [hep-ph]
2. *"Higgs Couplings at the End of 2012"* G. Belanger, B. Dumont, U. Ellwanger, J. F. Gunion and S. Kraml. arXiv:1212.5244 [hep-ph]

NMSSM Collaborators: G. Belanger, U. Ellwanger, Y. Jiang, S. Kraml, J. Schwarz

1. *"Higgs Bosons at 98 and 125 GeV at LEP and the LHC"* G. Belanger, U. Ellwanger, J. F. Gunion, Y. Jiang, S. Kraml and J. H. Schwarz. arXiv:1210.1976 [hep-ph]
2. *"Two Higgs Bosons at the Tevatron and the LHC?"* G. Belanger, U. Ellwanger, J. F. Gunion, Y. Jiang and S. Kraml. arXiv:1208.4952 [hep-ph]
3. *"Diagnosing Degenerate Higgs Bosons at 125 GeV"* J. F. Gunion, Y. Jiang and S. Kraml. arXiv:1208.1817 [hep-ph]

4. *"Could two NMSSM Higgs bosons be present near 125 GeV?"* J. F. Gunion, Y. Jiang and S. Kraml. arXiv:1207.1545 [hep-ph]
5. *"The Constrained NMSSM and Higgs near 125 GeV"* J. F. Gunion, Y. Jiang and S. Kraml. arXiv:1201.0982 [hep-ph] Phys. Lett. B **710**, 454 (2012)

2HDM Collaborators: Alexandra Drozd, Bohdan Grzadkowski, Yun Jiang

1. *"Two-Higgs-Doublet Models and Enhanced Rates for a 125 GeV Higgs"* A. Drozd, B. Grzadkowski, J. F. Gunion and Y. Jiang. arXiv:1211.3580 [hep-ph]

How do we see the Higgs boson?

- **The SM Higgs field was introduced to give mass to all elementary particles, especially the electroweak gauge bosons, $W^\pm$ and Z. It must be a $SU(2)$ doublet: $\begin{pmatrix} \rho^+ \\ \frac{1}{\sqrt{2}}(v + H + i\rho^0) \end{pmatrix}$.**
  v is the Higgs field vacuum expectation value (vev); ρ^+, ρ^0 are "eaten" to give m_W, m_Z.
  H is the remaining observable quantum fluctuation called the Higgs boson.
- **Since the Higgs field gives mass, the Higgs boson H couples to elementary particles proportionally to their mass:**

$$\begin{aligned} \mathcal{L} &= g\Big[C_V\left(m_W W_\mu W^\mu + \frac{m_Z}{\cos\theta_W} Z_\mu Z^\mu\right) \\ &\quad - C_U \frac{m_t}{2m_W}\bar{t}t - C_D \frac{m_b}{2m_W}\bar{b}b - C_D \frac{m_\tau}{2m_W}\bar{\tau}\tau\Big] H \,. \end{aligned} \tag{1}$$

  where $C_U = C_D = C_V = 1$ in the SM.
- **In addition to these "tree-level" couplings there are also loop-induced couplings $gg \to H$ and $\gamma\gamma \to H$, the former dominated by the top-quark loop and the latter dominated by the W loop with a smaller and opposite contribution from a top-quark loop.**
- **Because of the Higgs mass being $\sim 125~\mathrm{GeV}$, there is a remarkable mixture of observable Higgs decays and observable cross sections.**

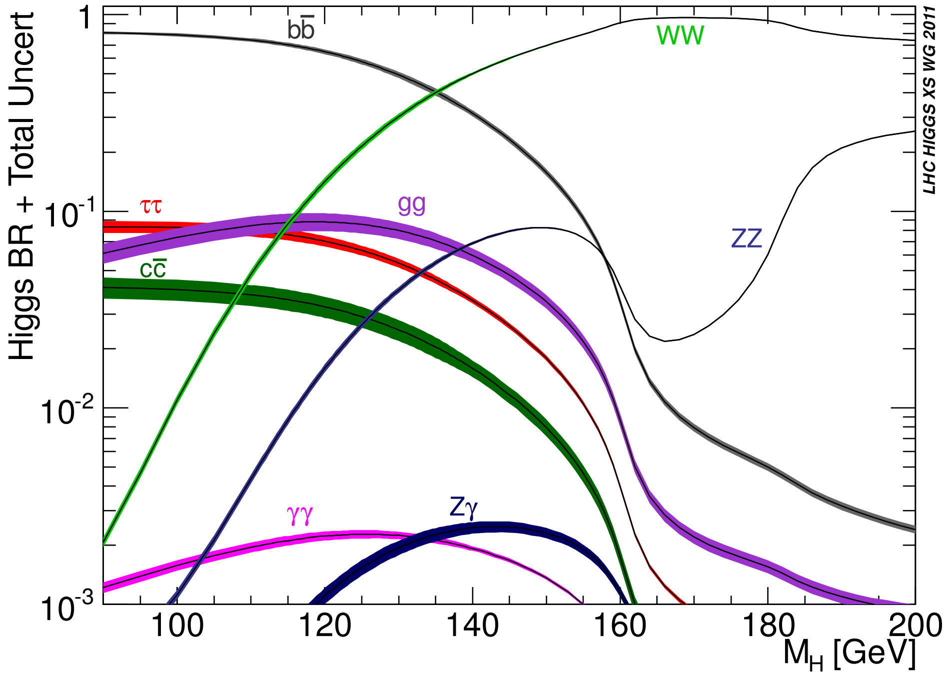

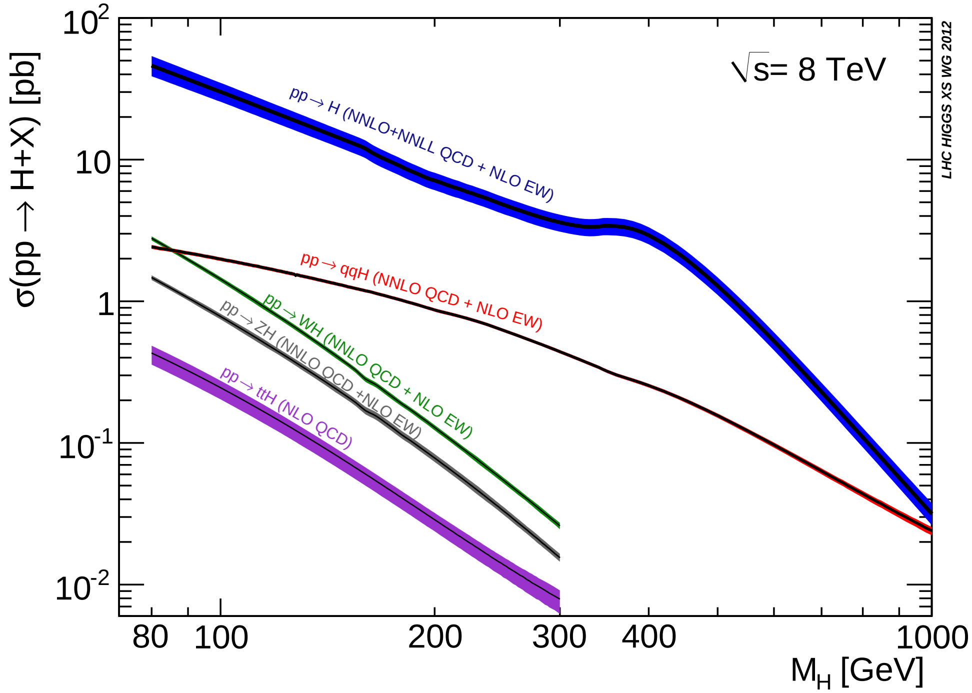

The most important ones for the initial discovery were those with very excellent mass resolution — the $H \to \gamma\gamma$ final state and the $H \to ZZ \to 4\ell$ final state.

In these final states you can actually see the resonance peak — see later.

- **The four key production and decay processes for the initial discovery were:**

$$\begin{array}{rl} gg \text{ fusion: ggF} & gg \to H \to \gamma\gamma; \quad gg \to H \to ZZ \to 4\ell \\ WW, ZZ \text{ fusion: VBF} & WW \to H \to \gamma\gamma; \quad WW \to H \to ZZ \to 4\ell \,, \end{array} \quad (2)$$

the gg induced processes having the highest rate. Sample diagrams for two of these processes are given below.

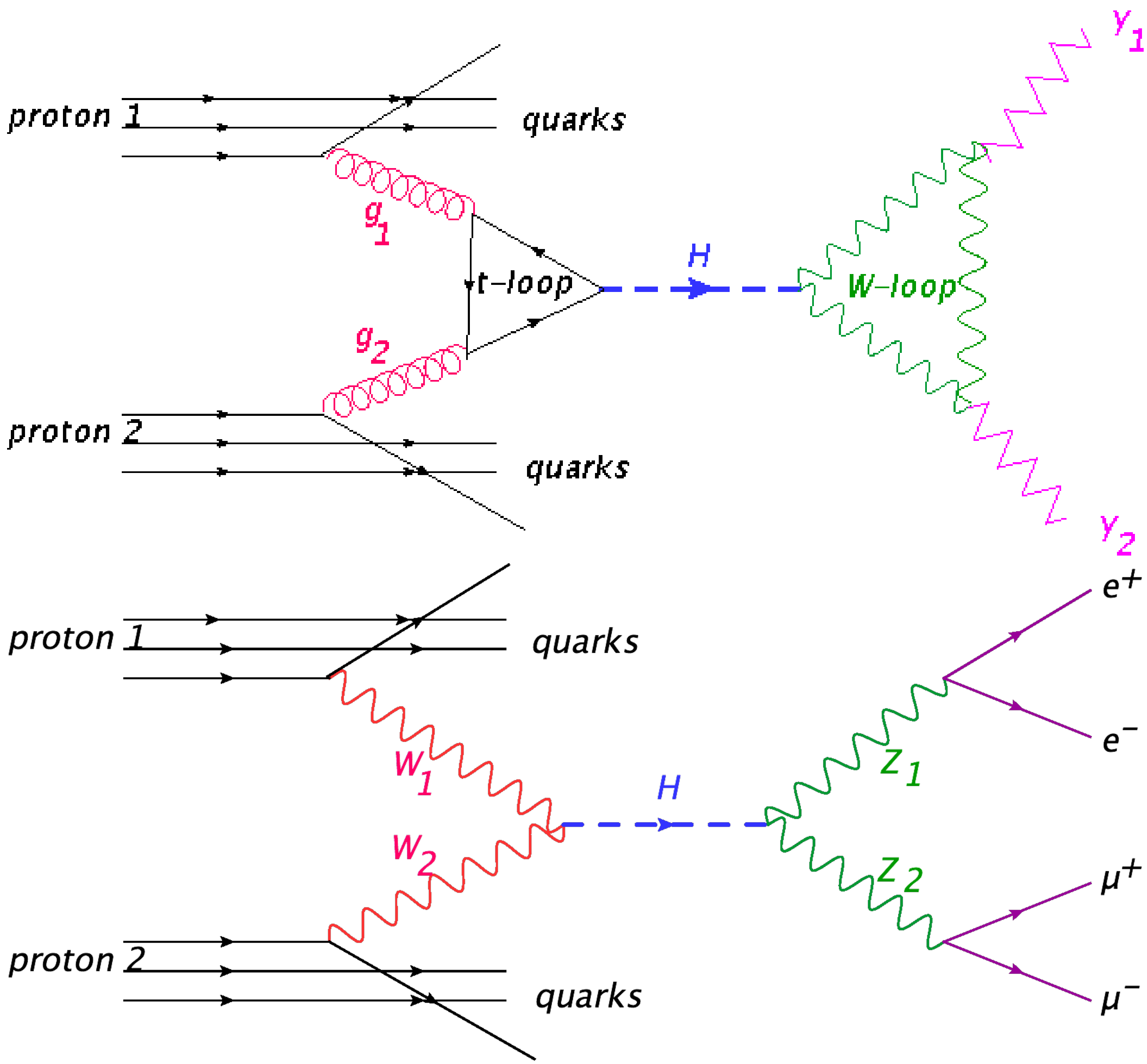

Figure 1: **Note the loops for the gg and $\gamma\gamma$ couplings in the upper figure.**

Gordy Kane, Jose Wudka and I anticipated the importance of these channels back in 1985 and pushed the detectors to have excellent electromagnetic calorimeters so that they could actually see the resonance peaks. 80 million dollars later we see:

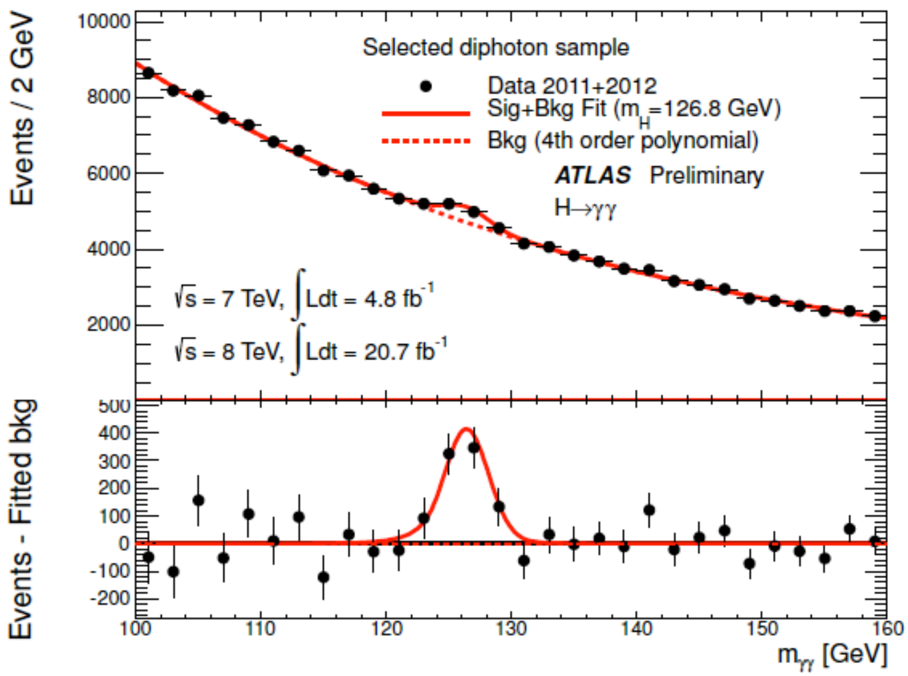

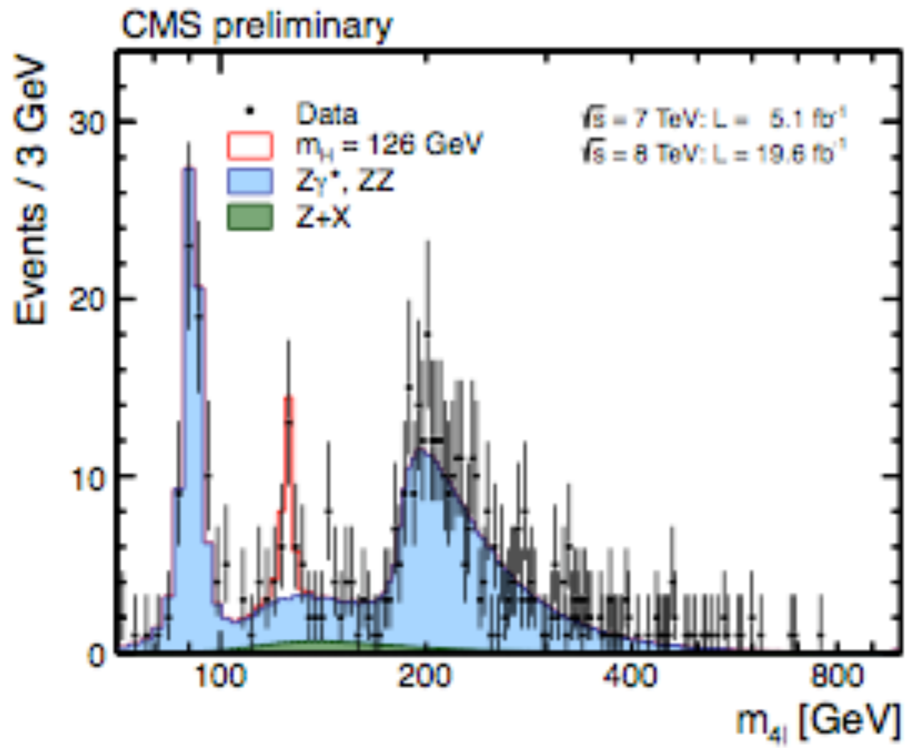

Basic Features of the Higgs-like LHC Excesses at $125 - 126$ GeV

- It is conventional to reference the SM expectations by defining the R ratios, called μ ratios by the experimentalists:

$$R^h_Y(X) = \frac{\sigma(pp \to Y \to h)\mathrm{BR}(h \to X)}{\sigma(pp \to Y \to h_{SM})\mathrm{BR}(h_{SM} \to X)}, \quad R^h(X) = \sum_Y R^h_Y, \qquad (3)$$

where $Y = gg$, VV, Vh or $t\bar{t}h$. The notation $\mu \equiv R$ is employed by the experimental groups.

A brief summary:

– ATLAS sees $\mu_{\mathrm{ggF}}(\gamma\gamma) > 1$ and $\mu_{\mathrm{VBF}}(\gamma\gamma) > 1$.
– CMS MVA analysis finds $\mu_{\mathrm{ggF}}(\gamma\gamma) < 1$, although still within errors of the SM value of 1. However, they do find $\mu_{\mathrm{VBF}}(\gamma\gamma) > 1$.
– ATLAS sees $\mu_{\mathrm{ggF}}(4\ell) > 1$ and $\mu_{\mathrm{VBF}}(4\ell) > 1$.
– CMS MVA analysis yields very SM-like values for the $ZZ \to 4\ell$ rates in ggF and VBF.

Sample plots are:

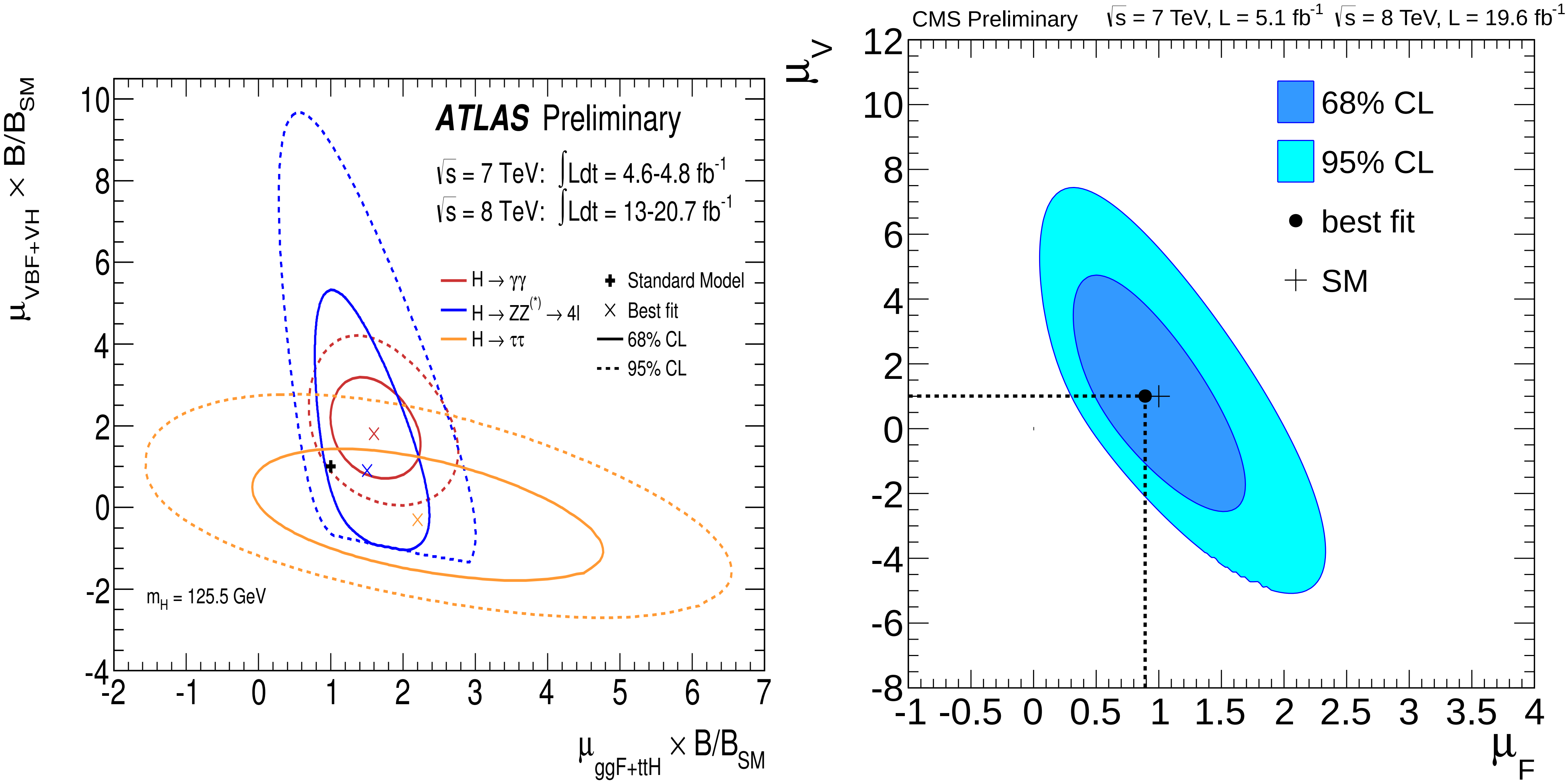

Figure 2: Left: ATLAS results, including 4ℓ and $\gamma\gamma$. Right: CMS results for 4ℓ. Vertical axis is VBF and horizontal is ggF.

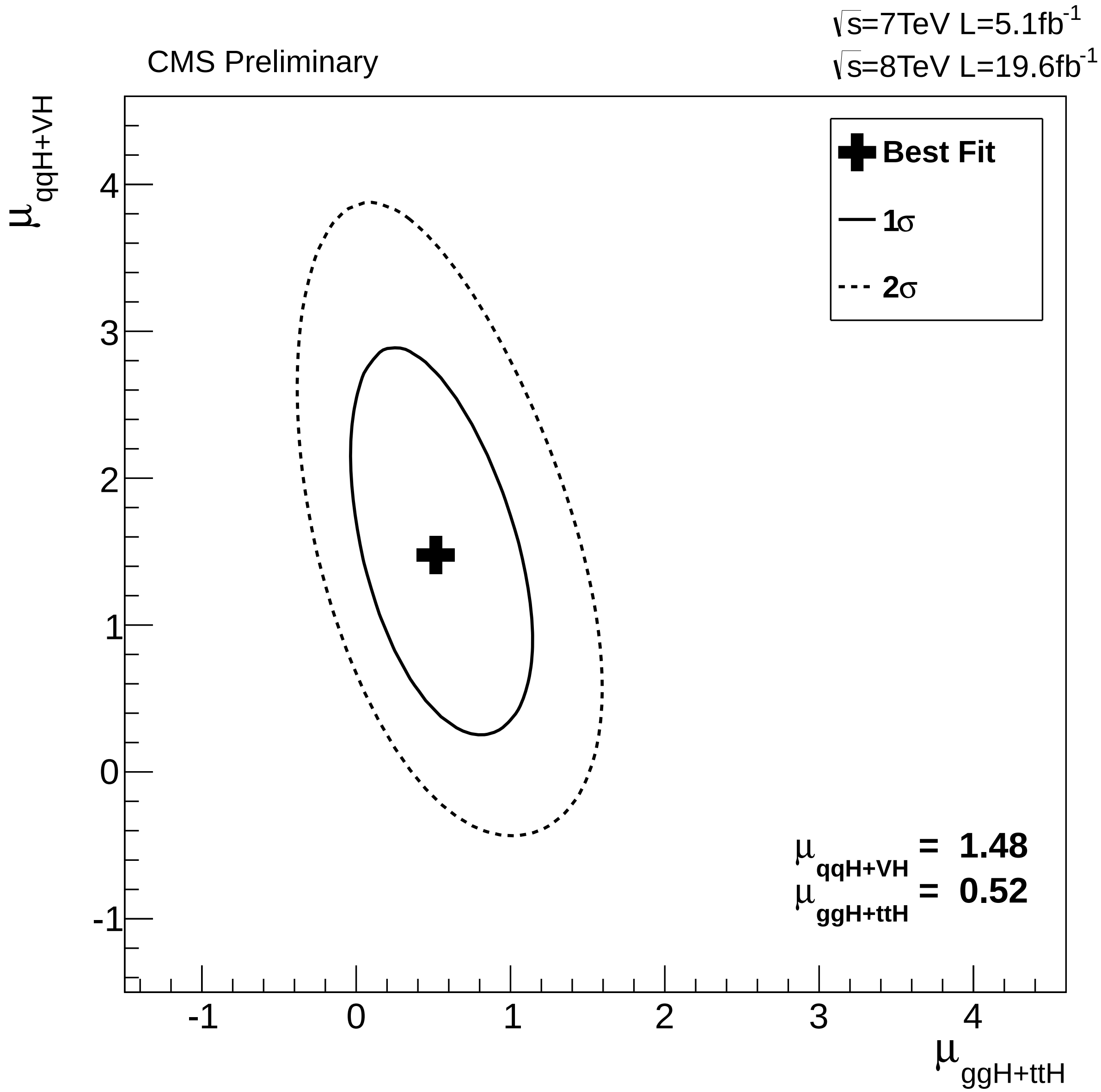

Figure 3: CMS MVA results for $\gamma\gamma$. Vertical axis is VBF and horizontal is ggF. Note $\mu_{\rm ggF} < 1$ bu $\mu_{\rm VBF} > 1$.

On the other hand there is a 2nd CMS analysis that gives a larger $\gamma\gamma$ signal. Compare:

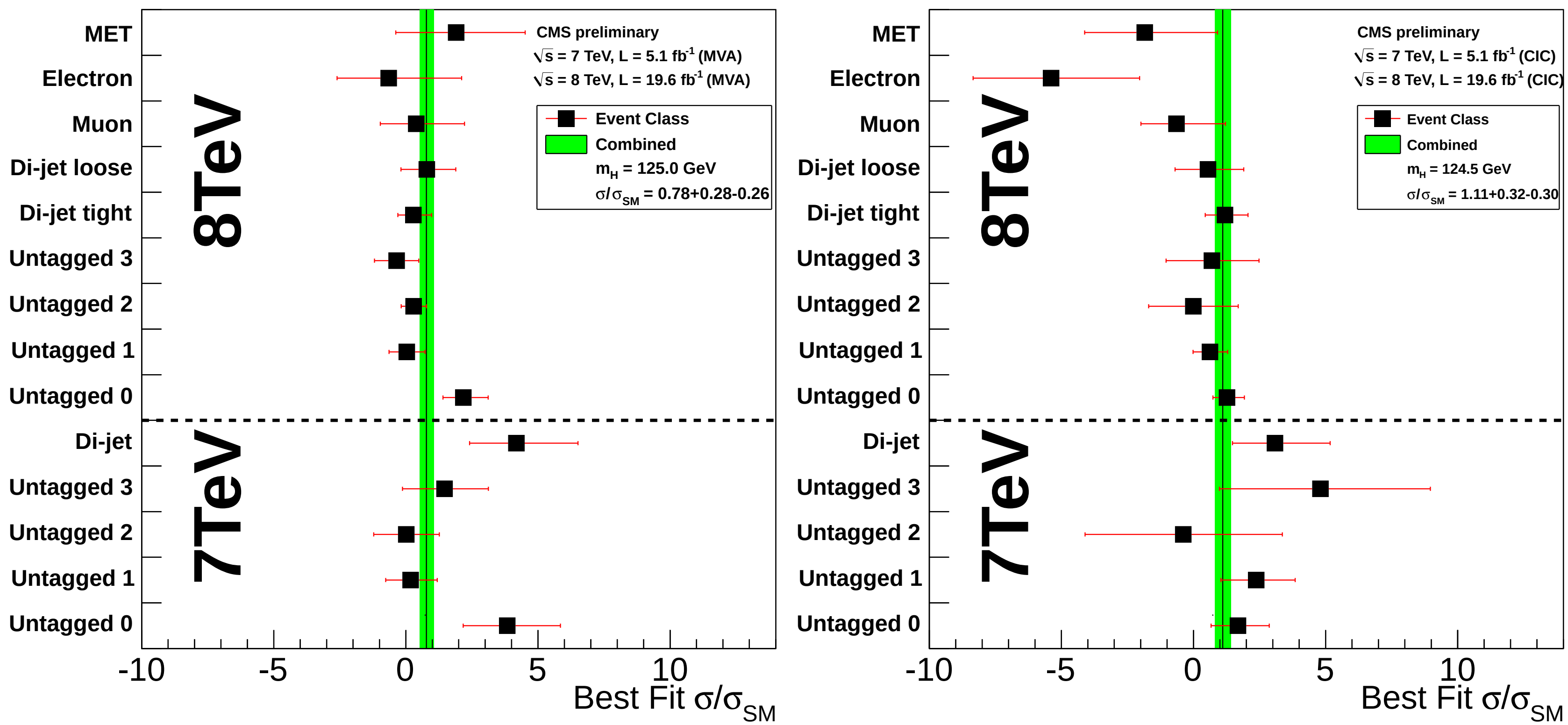

Figure 4: Left: MVA analysis results with overall $\mu = 0.78$. Right: CiC (cut-based) analysis results. CiC analysis shows overall enhancement in $\gamma\gamma$ of $\mu = 1.11$. CMS quotes a discrepancy of 1.8σ between the two analyses.

- **The big questions:**
  1. **If the deviations from a single SM Higgs survive what is the model?**

     And, how far beyond the ”standard” model must we go to describe them?
  2. **If all results become SM-like, how can we be sure that we are seeing just a SM-like Higgs boson?**

     Yes, there are complicated Higgs models that can give SM-like rates for most, or even all, channels.

Higgs coupling fits

- Suppose the signal derives from just one Higgs boson — we assume 0^+.
- The structure we will test is that given earlier:

$$\mathcal{L} = g\Big[C_V\left(m_W W_\mu W^\mu + \frac{m_Z}{\cos\theta_W} Z_\mu Z^\mu\right) - C_U\frac{m_t}{2m_W}\bar{t}t - C_D\frac{m_b}{2m_W}\bar{b}b - C_D\frac{m_\tau}{2m_W}\bar{\tau}\tau\Big]H\,. \quad (4)$$

In general, the C_I can take on negative as well as positive values; there is one overall sign ambiguity which we fix by taking $C_V > 0$.

- We will be fitting the data summarized earlier (using CMS MVA analysis results for $\gamma\gamma$).

- In addition to the tree-level couplings given above, the H has couplings to gg and $\gamma\gamma$ that are first induced at one loop and are completely computable in terms of C_U, C_D and C_V if only loops containing SM particles are present.

  We define $\overline{C}_g$ and $\overline{C}_\gamma$ to be the ratio of these couplings so computed to the SM ($i.e.$ $C_U = C_D = C_V = 1$) values.
- However, in some of our fits we will also allow for additional loop contributions ΔC_g and ΔC_γ from new particles; in this case $C_g = \overline{C}_g + \Delta C_g$ and $C_\gamma = \overline{C}_\gamma + \Delta C_\gamma$.
- The largest set of independent parameters that we might wish to consider is thus:

$$C_U,\ C_D,\ C_V,\ \Delta C_g,\ \Delta C_\gamma\,. \tag{5}$$

- **Fit I: $C_U = C_D = C_V = 1$, ΔC_g and ΔC_γ free.**

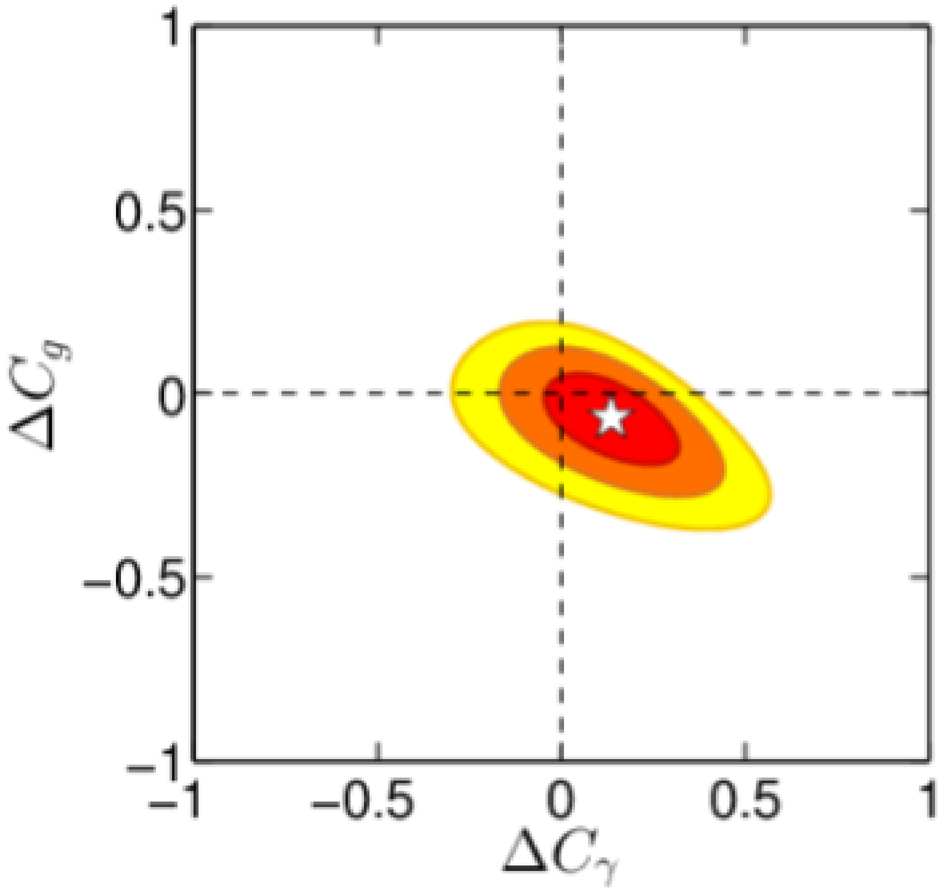

Figure 5: Two parameter fit of ΔC_γ and ΔC_g, assuming $C_U = C_D = C_V = 1$ (Fit I). The red, orange and yellow ellipses show the 68%, 95% and 99.7% CL regions, respectively. The white star marks the best-fit point. Looking quite SM-like when all ATLAS and CMS data are combined.

- **Fit II: varying C_U, C_D and C_V ($\Delta C_\gamma = \Delta C_g = 0$)**

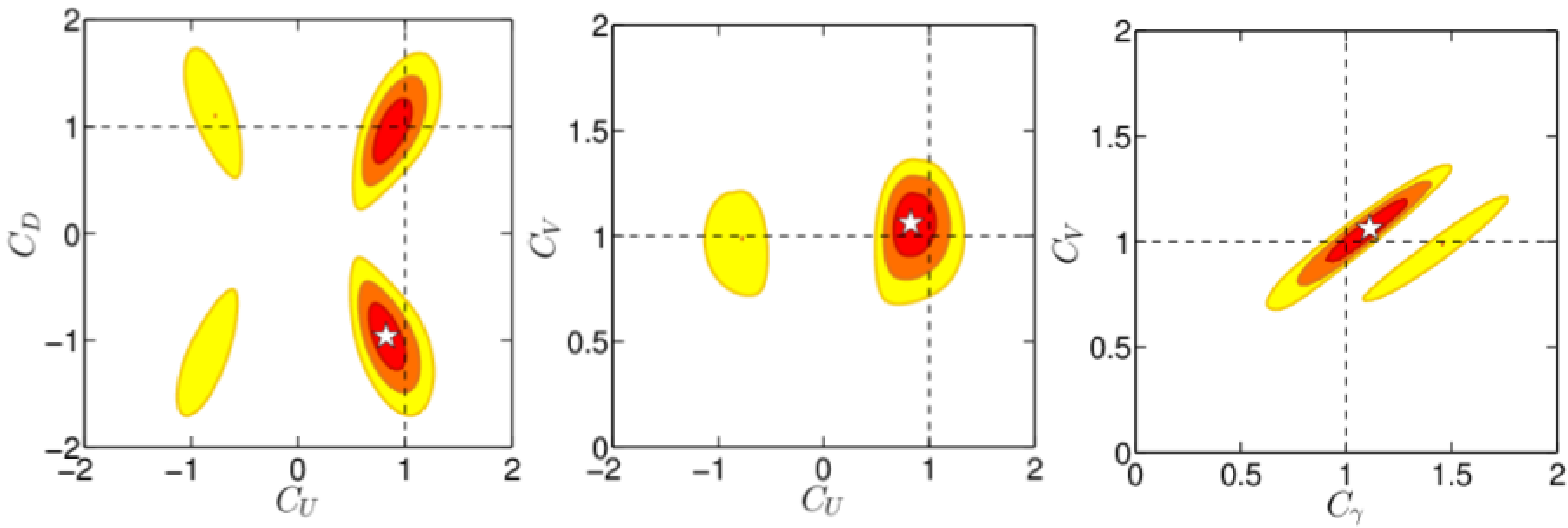

Figure 6: Two-dimensional χ^2 distributions for the three parameter fit, Fit II, of C_U, C_D, C_V with $C_\gamma = \overline{C}_\gamma$ and $C_g = \overline{C}_g$ as computed in terms of C_U, C_D, C_V. Unlike earlier fits that did not include CMS MVA $\gamma\gamma$ results, $C_U > 0$ is now preferred since overall there is no $\gamma\gamma$ enhancement in ggF after "averaging" ATLAS and CMS.

Fit	Standard Model	ΔC_γ, ΔC_g	C_U, C_D, C_V
$\chi^2_{\rm min}$ $\chi^2_{\rm min}$/d.o.f.	21.6 0.90	20.1 0.91	19.9 0.94
dominant contributions to $\chi^2_{\rm min}$	ATLAS $\gamma\gamma$ Tevatron $\gamma\gamma$ ATLAS ZZ	ATLAS ZZ CMS $\gamma\gamma$ ATLAS $\gamma\gamma$	ATLAS $\gamma\gamma$ CMS WW VBF Tevatron $\gamma\gamma$

- **There is no improvement in $\chi^2/d.o.f.$ as freedom is introduced, *i.e.* the lowest p value is achieved in the SM!**

  Allowing all five parameters, $C_U, C_D, C_V, \Delta C_\gamma, \Delta C_g$ to vary again worsens the p value, unlike earlier "end of 2012" fits.
- **Thus, perhaps there is no need for a mechanism that would yield enhanced $\mu = R$ values.**

  However, the fits above only reflect some average properties and it could be that individual channels (*e.g.* the VBF$\rightarrow H \rightarrow \gamma\gamma$) will in the end turn out to be enhanced.

Multiple Higgs Models

- Let us suppose that the "final" results for the Higgs signals cannot be fit by the SM Higgs.

  At the moment there are many hints that this could be the case despite the fact that the average result is close to SM-like.
- This would make it natural to consider models in which there is more than one Higgs boson. Some Higgs could dominate one kind of signal and other Higgs could dominate another kind of signal. Such models include:

  1. Two-Higgs Doublet Models (2HDM)

     In this model the one-doublet complex Higgs field of the SM is replicated and each of the neutral components of the two doublet fields acquires a vacuum expectation value: we have v_1 and v_2.

An important parameter of such a model is is $\tan\beta = v_2/v_1$ — $v_1^2 + v_2^2 = v^2 = (246~\mathrm{GeV})^2$ is required to get the W, Z masses right.

2 complex doublets have 8 degrees of freedom, of which only 3 are absorbed or "eaten" in giving the $W^\pm, Z$ their masses. The remaining 5 d.o.f. become physical scalar particles:

$$\text{CP-even}: \; h, H\,, \quad \text{CP-odd}: \; A\,, \quad \text{charged pair}: \; H^\pm \tag{6}$$

2. Minimal Supersymmetric Model (MSSM)

   The Higgs sector is just a constrained version of the 2HDM model category. No additional Higgs bosons. However, the SUSY constraints are such that it hard to get a CP-even Higgs boson with SM-like properties without going to extremes.

3. Adding additional doublets to the 2HDM or MSSM

Makes a mess of gauge coupling unification in the MSSM case.

4. **Adding additional singlets to a 2HDM or the MSSM**

   Every additional complex singlet yields one more CP-even H and one more CP-odd A.

   No impact on gauge unification since it is a *singlet* that is being added.

   – A particularly attractive version is the Next-to-Minimal Supersymmetric Model (NMSSM).

     Getting the lightest CP-even Higgs to be as heavy as $125~\mathrm{GeV}$ does not require extremes. It is an altogether beautiful model.

Enhanced Higgs signals in the NMSSM

- **NMSSM=MSSM+$\widehat{S}$.**
- **The extra complex S component of $\widehat{S}$ $\Rightarrow$ the NMSSM has h_1, h_2, h_2, a_1, a_2.**
- **The new NMSSM parameters of the superpotential (λ and κ) and scalar potential (A_λ and A_κ) appear as:**

$$W \ni \lambda \widehat{S}\widehat{H}_u\widehat{H}_d + \frac{\kappa}{3}\widehat{S}^3, \quad V_{\rm soft} \ni \lambda A_\lambda S H_u H_d + \frac{\kappa}{3}A_\kappa S^3 \quad (7)$$

- **$\langle S\rangle \neq 0$ is generated by SUSY breakng and solves μ problem: $\mu_{\rm eff} = \lambda\langle S\rangle$.**
- **First question: Can the NMSSM give a Higgs mass as large as $125~\mathrm{GeV}$?**

  Answer: Yes, so long as parameters at the GUT scale are not fully unified. For our studies, we employed universal

m_0, except for NUHM ($m_{H_u}^2$, $m_{H_d}^2$, m_S^2 free), universal $A_t = A_b = A_\tau = A_0$ but allow A_λ and A_κ to vary freely. Of course, $\lambda > 0$ and κ are scanned demanding perturbativity up to the GUT scale.

- Can this model achieve rates in $\gamma\gamma$ and 4ℓ that are $>$SM?
  Answer: It depends on whether or not we require a good prediction for the muon anomalous magnetic moment, a_μ.
- The possible $R(\gamma\gamma) > 1$ mechanism (arXiv:1112.3548, Ellwanger) is to reduce the $b\bar{b}$ width of the mainly SM-like Higgs by giving it some singlet component. The gg and $\gamma\gamma$ couplings are less affected.
- Typically, this requires m_{h_1} and m_{h_2} to have similar masses (for singlet-doublet mixing) and large λ (to enhance Higgs mass).
  Large λ (by which we mean $\lambda > 0.1$) is only possible while retaining perturbativity up to m_{Pl} if $\tan\beta$ is modest in size.
  In the semi-unified model we employ, enhanced rates and/or

large λ cannot be made consistent with decent δa_μ. (J. F. Gunion, Y. Jiang and S. Kraml.arXiv:1201.0982 [hep-ph])

- **Some illustrative R_{gg} results from** (J. F. Gunion, Y. Jiang and S. Kraml. arXiv:1207.1545):

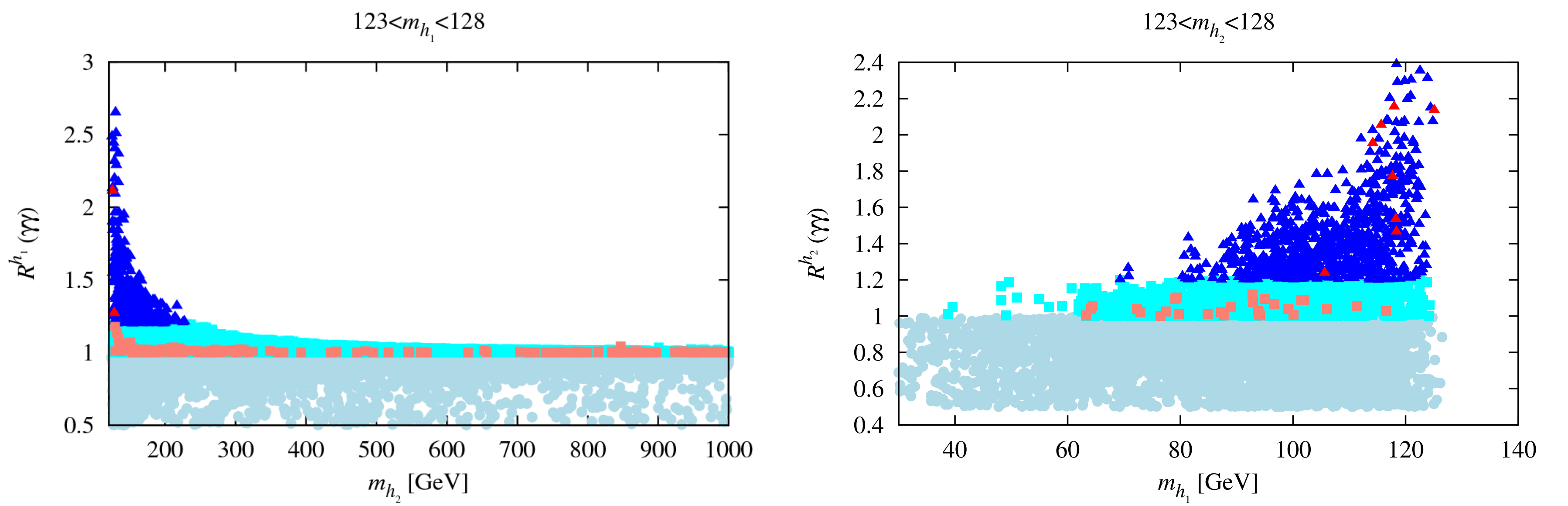

Figure 7: The plot shows $R_{gg}(\gamma\gamma)$ for the cases of $123 < m_{h_1} < 128~\mathrm{GeV}$ and $123 < m_{h_2} < 128~\mathrm{GeV}$. Note: red triangle (orange square) is for WMAP window with $R_{gg}(\gamma\gamma) > 1.2$ ($R_{gg}(\gamma\gamma) = [1, 1.2]$).

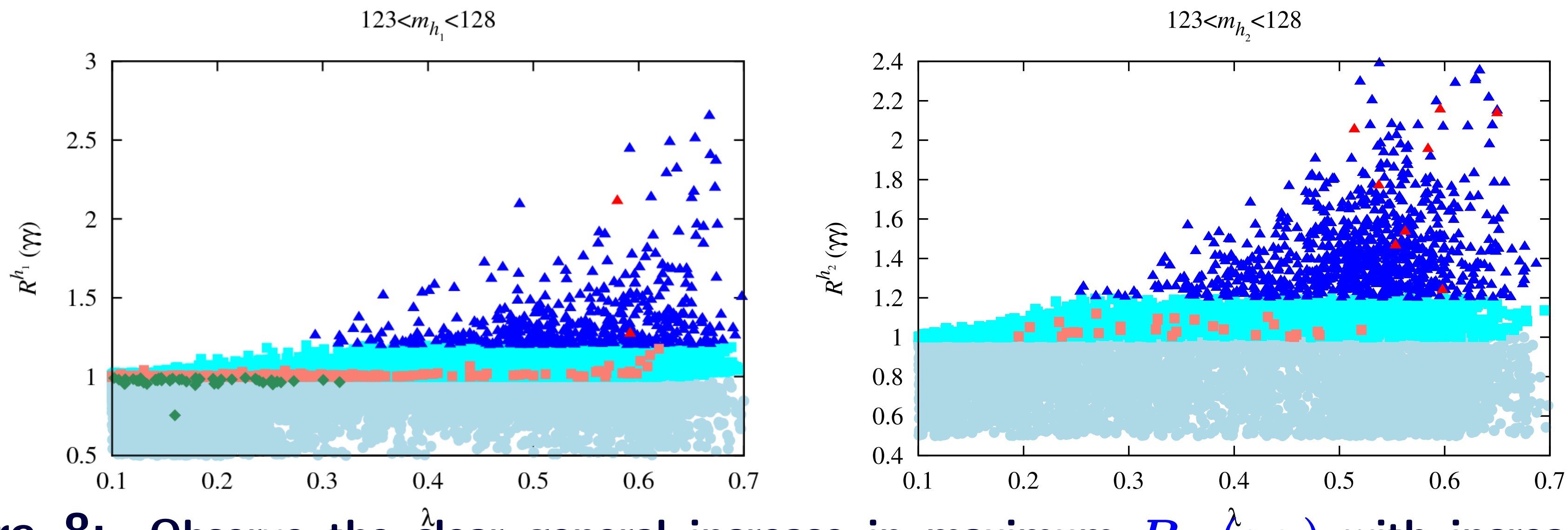

Figure 8: Observe the clear general increase in maximum $R_{gg}(\gamma\gamma)$ with increasing λ. Green points have good δa_μ, $m_{h_2} > 1$ TeV BUT $R_{gg}(\gamma\gamma) \sim 1$.

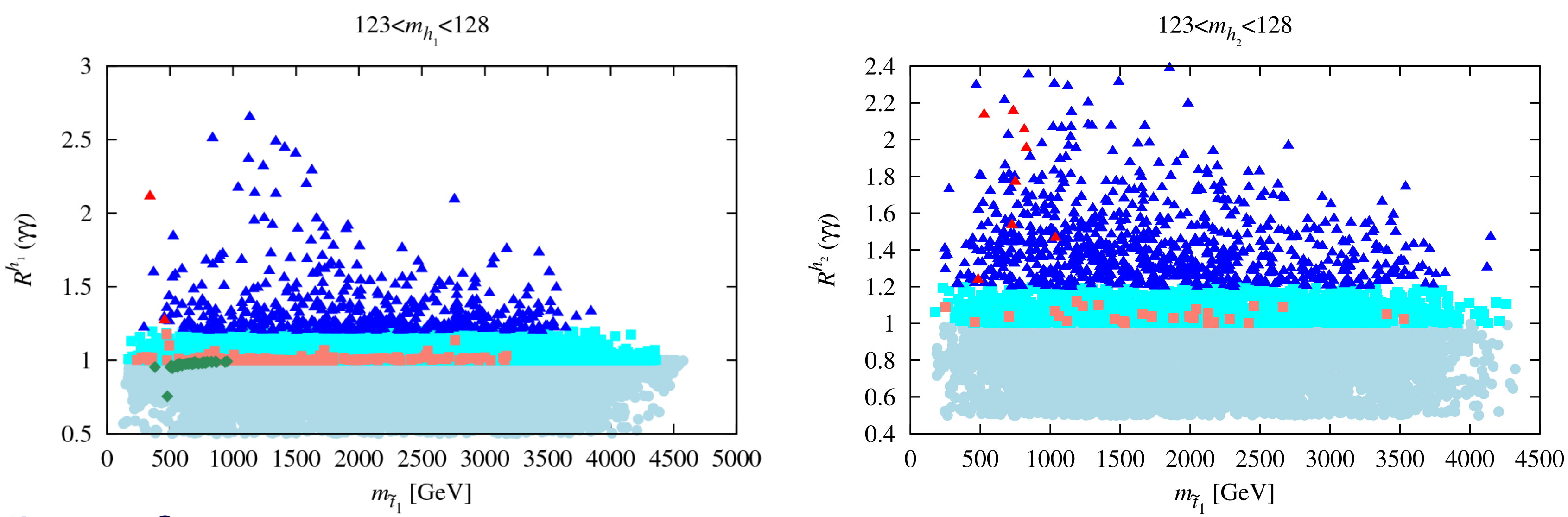

Figure 9: The lightest stop has mass $\sim 300 - 700$ GeV for red-triangle points.

- If we ignore δa_μ, then $R_{gg}(\gamma\gamma) > 1.2$ (even > 2) is possible while satisfying all other constraints provided h_1 and h_2 are close in mass, especially in the case where $m_{h_2} \in [123, 128]$ GeV window.
- This raises the issue of scenarios in which *both* m_{h_1} and m_{h_2} are in the $[123, 128]$ GeV window where the experiments see the Higgs signal.

The ideas and issues related to degeneracy:

- If h_1 and h_2 are sufficiently degenerate, the experimentalists might not have resolved the two distinct peaks, even in the $\gamma\gamma$ channel.
- The rates for the h_1 and h_2 could then add together to give an enhanced $\gamma\gamma$ signal.
- The apparent width or shape of the $\gamma\gamma$ mass distribution could be altered.
- There is more room for an apparent mismatch between the

$\gamma\gamma$ channel and other channels, such as $b\bar{b}$ or 4ℓ, than in non-degenerate situation.
In particular, the h_1 and h_2 will generally have different gg and VV production rates and branching ratios.

Degenerate NMSSM Higgs Scenarios:

(arXiv:1207.1545, JFG, Jiang, Kraml)

- **For the numerical analysis, we used NMSSMTools version 3.2.0, which has improved convergence of RGEs in the case of large Yukawa couplings.**
- **The precise constraints imposed are the following.**

1. **Basic constraints: proper RGE solution, no Landau pole, neutralino LSP, Higgs and SUSY mass limits as implemented in NMSSMTools-3.2.0.**
2. B **physics:**
3. **Dark Matter:** $\Omega h^2 < 0.136$ **— allows for scenarios in which the relic density arises in part from some other source. However, we single out points with** $0.094 \leq \Omega h^2 \leq 0.136$**, which is the 'WMAP window' defined in NMSSMTools-3.2.0.**
4. **2011 XENON100: spin-independent LSP–proton scattering**

cross section bounds implied by the neutralino-mass-dependent XENON100 bound. (2012 XENON100 has little additional impact.)

5. δa_μ ignored: impossible to satisfy for scenarios studied here.

- Compute the effective Higgs mass in given production and final decay channels Y and X, respectively, and R^h_{gg} as

$$m_h^Y(X) \equiv \frac{R_Y^{h_1}(X) m_{h_1} + R_Y^{h_2}(X) m_{h_2}}{R_Y^{h_1}(X) + R_Y^{h_2}(X)} \quad R_Y^h(X) = R_Y^{h_1}(X) + R_Y^{h_2}(X) \,. \tag{8}$$

- The extent to which it is appropriate to combine the rates from the h_1 and h_2 depends upon the degree of degeneracy and the experimental resolution. Very roughly, one should probably think of $\sigma_{\rm res} \sim 1.5~\mathrm{GeV}$ or larger. The widths of the h_1 and h_2 are very much smaller than this resolution.

- We only display points which pass constraints listed earlier, *and* have $123~\mathrm{GeV} < m_{h_1}, m_{h_2} < 128~\mathrm{GeV}$.

• **Many of the displayed points have $R^{h_1}_{gg}(\gamma\gamma) + R^{h_2}_{gg}(\gamma\gamma) > 1$.**

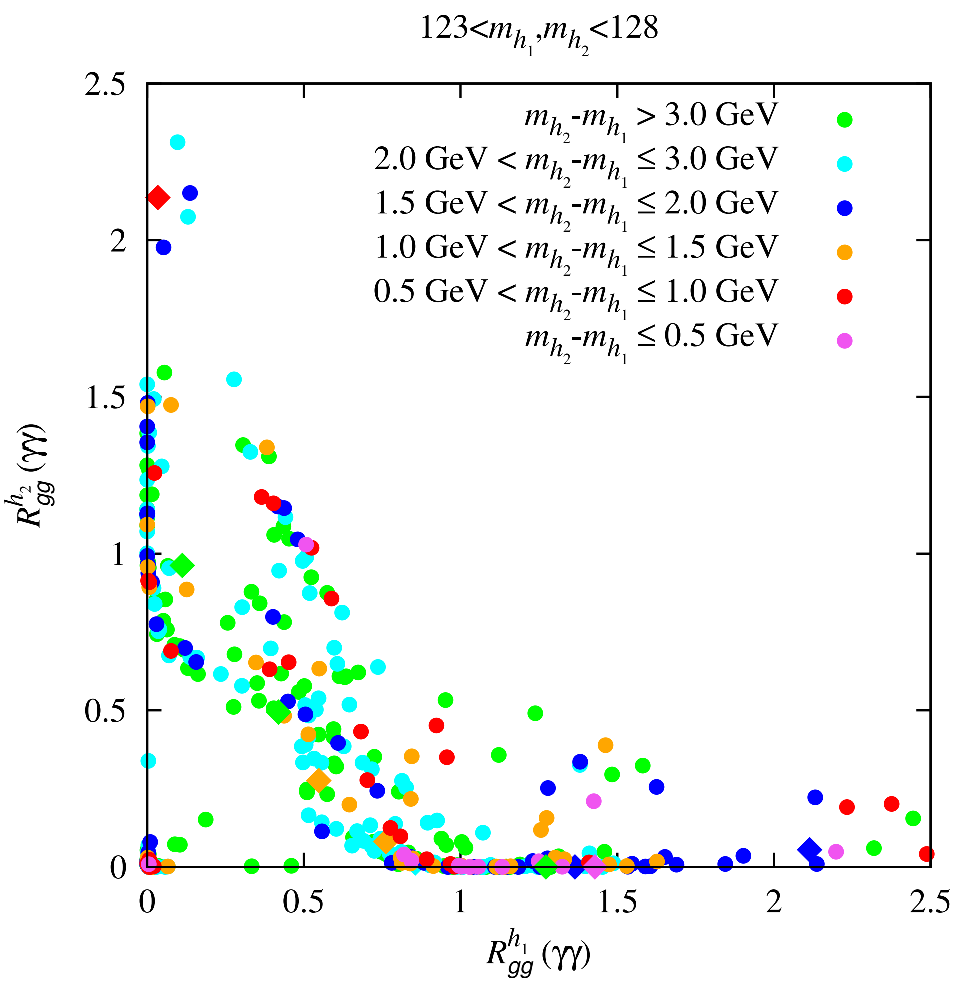

Figure 10: Correlation of $gg \to (h_1, h_2) \to \gamma\gamma$ signal strengths when both h_1 and h_2 lie in the 123–$128\ \mathrm{GeV}$ mass range. The circular points have $\Omega h^2 < 0.094$, while diamond points have $0.094 \leq \Omega h^2 \leq 0.136$. Points are color coded according to $m_{h_2} - m_{h_1}$. Probably green and cyan points can be resolved in mass.

Now combine the h_1 and h_2 signals. Color code:

1. red for $m_{h_2} - m_{h_1} \leq 1~\mathrm{GeV}$;
2. blue for $1~\mathrm{GeV} < m_{h_2} - m_{h_1} \leq 2~\mathrm{GeV}$;
3. green for $2~\mathrm{GeV} < m_{h_2} - m_{h_1} \leq 3~\mathrm{GeV}$.

- For current statistics and $\sigma_{\mathrm{res}} \gtrsim 1.5~\mathrm{GeV}$ we estimate that the h_1 and h_2 signals will not be seen separately for $m_{h_2} - m_{h_1} \leq 2~\mathrm{GeV}$.
- In Fig. 11, we show results for $R^h_{gg}(X)$ for $X = \gamma\gamma, VV, b\bar{b}$. Enhanced $\gamma\gamma$ and VV rates from gluon fusion are very common.
- The bottom-right plot shows that enhancement in Vh with $h \to b\bar{b}$ rate is also natural, though not as large as the best fit value suggested by the new Tevatron analysis.
- Diamond points ($i.e.$ those in the WMAP window) are rare, but typically show enhanced rates.

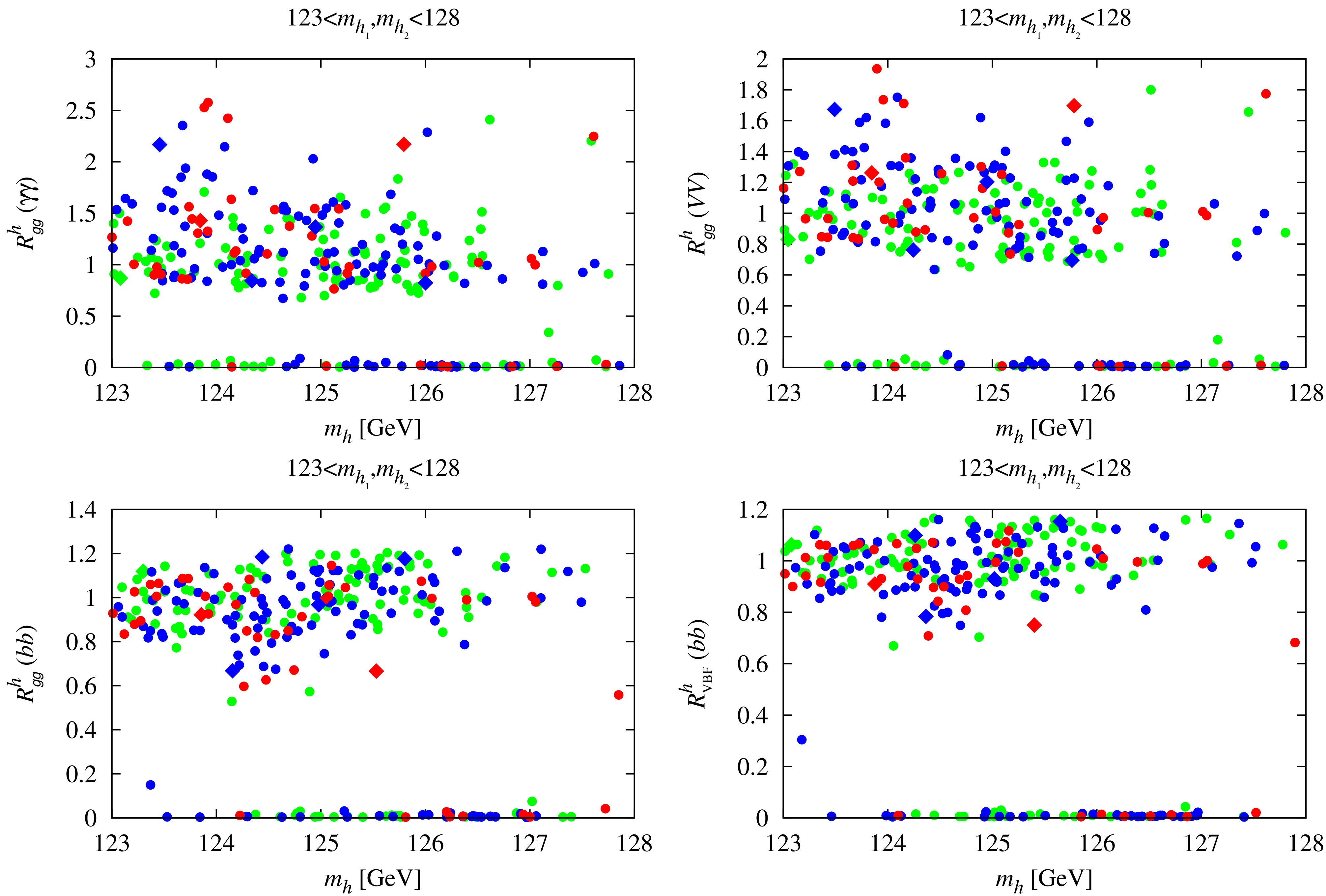

Figure 11: $R^h_{gg}(X)$ **for** $X = \gamma\gamma, VV, b\bar{b}$**, and** $R^h_{\rm VBF}(b\bar{b})$ **versus** m_h**. For application to the Tevatron, note that** $R^h_{\rm VBF}(b\bar{b}) = R^h_{V^*\to Vh}(b\bar{b})$**.**

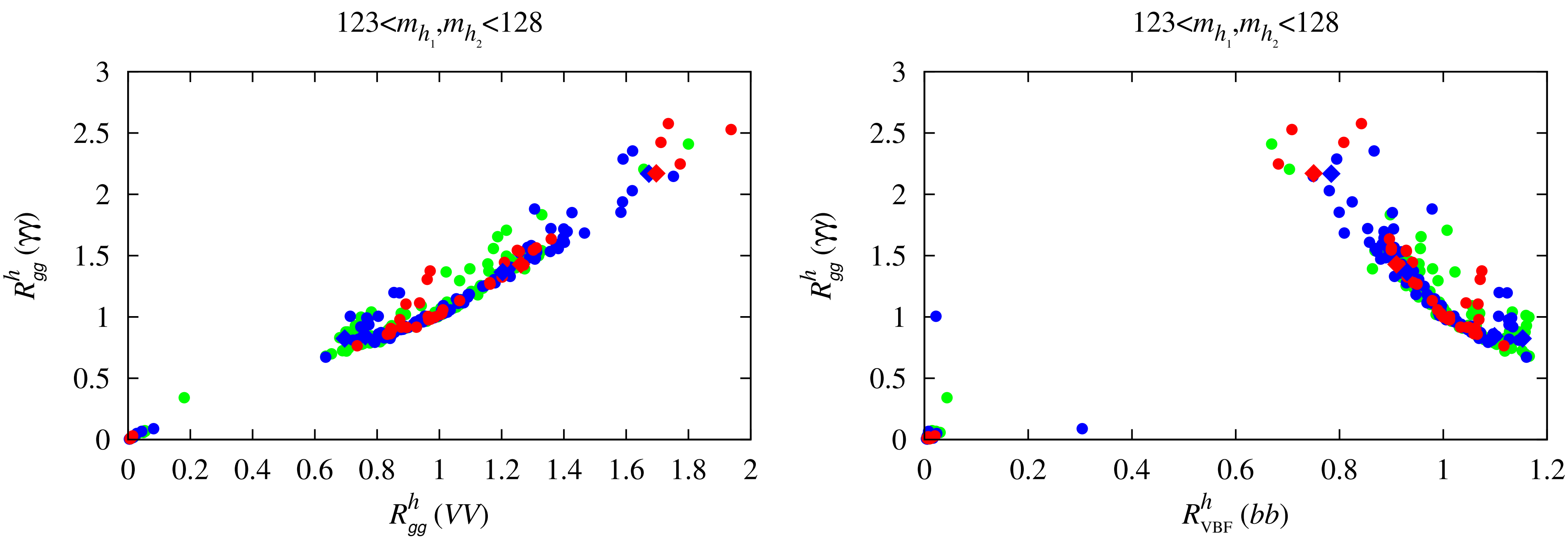

Figure 12: Left: correlation between the gluon fusion induced $\gamma\gamma$ and VV rates relative to the SM. Right: correlation between the gluon fusion induced $\gamma\gamma$ rate and the VV fusion induced $b\overline{b}$ rates relative to the SM; the relative rate for $V^* \to Vh$ with $h \to b\overline{b}$ (relevant for the Tevatron) is equal to the latter.

- **Comments on Fig. 12:**
  1. **Left-hand plot shows the strong correlation between $R^h_{gg}(\gamma\gamma)$ and $R^h_{gg}(VV)$.**

Note that if $R^h_{gg}(\gamma\gamma) \sim 1.3$ (as for ATLAS) then in this model $R^h_{gg}(VV) \geq 1$.

2. The right-hand plot shows the (anti) correlation between $R^h_{gg}(\gamma\gamma)$ and $R^h_{V^*\to Vh}(b\overline{b}) = R^h_{\mathrm{VBF}}(b\overline{b})$.
   In general, the larger $R^h_{gg}(\gamma\gamma)$ is, the smaller the value of $R^h_{V^*\to Vh}(b\overline{b})$.
3. It is often the case that one of the h_1 or h_2 dominates $R^h_{gg}(\gamma\gamma)$ while the other dominates $R^h_{V^*\to Vh}(b\overline{b})$.
   However, a significant number of the points are such that either the $\gamma\gamma$ or the $b\overline{b}$ signal receives substantial contributions from both the h_1 and the h_2.
   We did not find points where the $\gamma\gamma$ and $b\overline{b}$ final states *both* receive substantial contributions from *both* the h_1 and h_2.

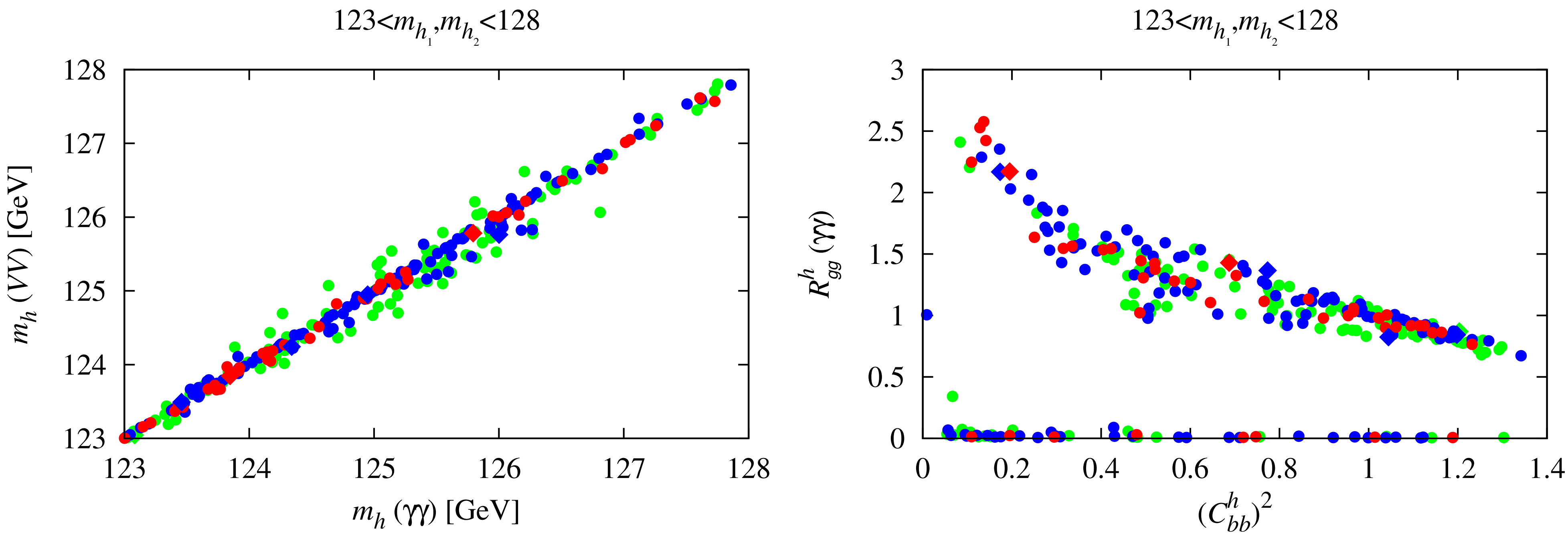

Figure 13: **Left: effective Higgs masses obtained from different channels: $m_h^{gg}(\gamma\gamma)$ versus $m_h^{gg}(VV)$. Right: $\gamma\gamma$ signal strength $R^h_{gg}(\gamma\gamma)$ versus effective coupling to $b\bar{b}$ quarks $(C^h_{b\bar{b}})^2$. Here, ${C^h_{b\bar{b}}}^2 \equiv \left[R^{h_1}_{gg}(\gamma\gamma){C^{h_1}_{b\bar{b}}}^2 + R^{h_2}_{gg}(\gamma\gamma){C^{h_2}_{b\bar{b}}}^2\right] / \left[R^{h_1}_{gg}(\gamma\gamma) + R^{h_2}_{gg}(\gamma\gamma)\right]$.**

Comments on Fig. 13

1. **The m_h values for the gluon fusion induced $\gamma\gamma$ and VV cases are also strongly correlated — in fact, they differ by**

no more than a fraction of a GeV and are most often much closer, see the left plot of Fig. 13.

2. The right plot of Fig. 13 illustrates the mechanism behind enhanced rates, namely that large net $\gamma\gamma$ branching ratio is achieved by reducing the average total width by reducing the average $b\bar{b}$ coupling strength.

- Although we have emphasized that degeneracy can easily lead to enhanced signals, it is equally true that a pair of degenerate Higgs could easily yield a SM-like signal.

  For example, points with $R_{gg}(\gamma\gamma) \sim 1$ are easily found in Fig. 10. And, Fig. 11 shows that other rates will often be SM-like at the same time.

- Either way, an important question is: how can we check for underlying degeneracy? This will be discussed later.

Separate Mass Peaks for ZZ vs. $\gamma\gamma$

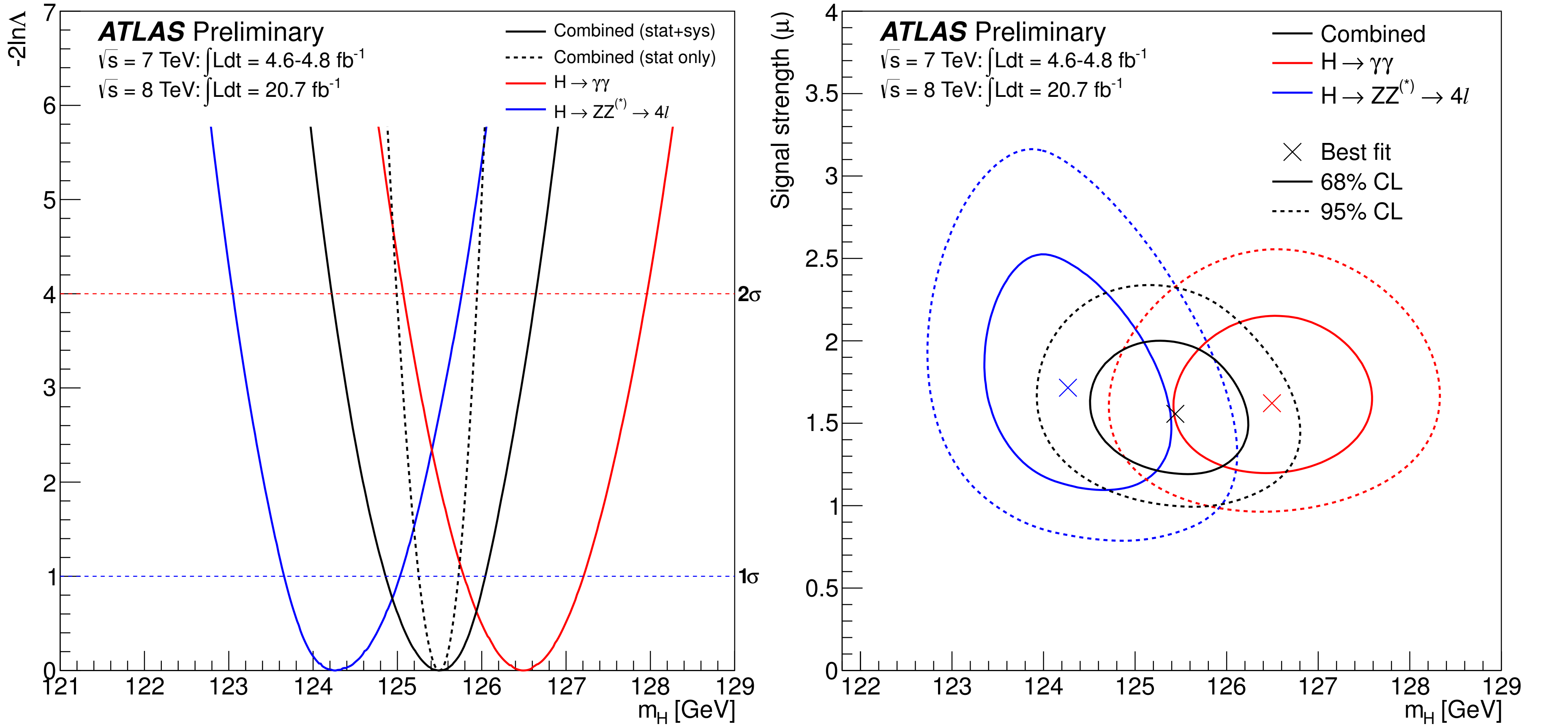

- h_1 **should have** $m_{h_1} \sim 124.2~\mathrm{GeV}$ **and** ZZ **rate not too much smaller than SM-like rate, but suppressed** $\gamma\gamma$ **rate.**
- h_2 **should have** $m_{h_2} \sim 126.5~\mathrm{GeV}$**, enhanced** $\gamma\gamma$ **rate and somewhat suppressed** ZZ **rate.**

- **The kind of extreme apparently seen by ATLAS is hard to arrange in the NMSSM.**

  This is because the mechanism for getting enhanced $\gamma\gamma$ **(suppression of** bb **partial width through mixing) automatically also enhances** ZZ**. Recall the correlation plot given earlier**

- **To assess a bit more quantitatively, we compute** $m_h(VV)$ **vs.** $m_h(\gamma\gamma)$ **using previous formula involving weighting by** $R_{gg}^{h_1,h_2}(ZZ)$ **and** $R_{gg}^{h_1,h_2}(\gamma\gamma)$ **and accepting points with** $121~\mathrm{GeV} \leq m_{h_1}, m_{h_2} \leq 128~\mathrm{GeV}$**.**

  Or, selecting points with $122~\mathrm{GeV} < m_{h_1} < 124~\mathrm{GeV}$ **and** $125~\mathrm{GeV} < m_{h_2} < 127~\mathrm{GeV}$**.**

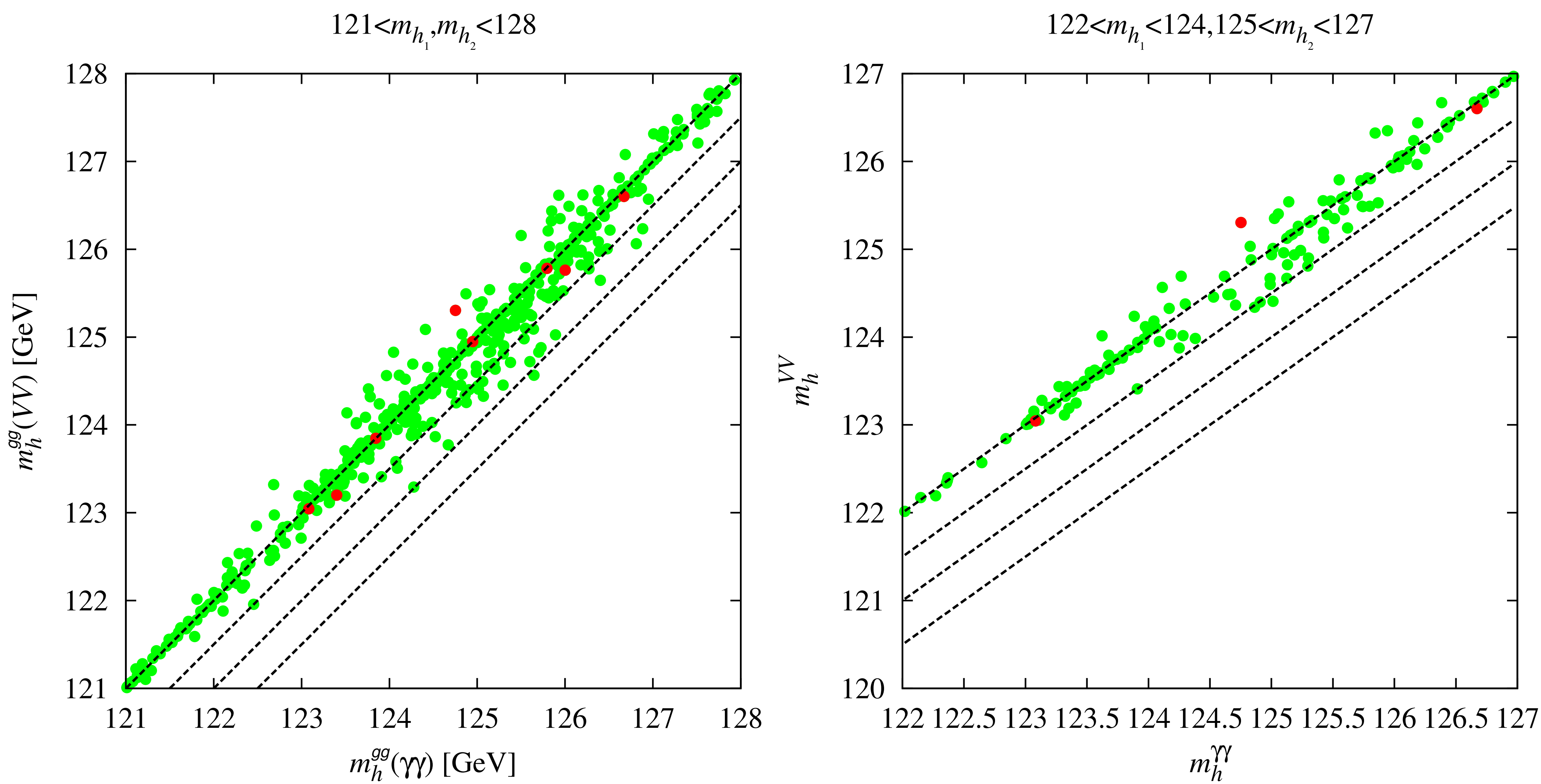

Figure 14: m_h obtained in ZZ vs. $\gamma\gamma$ final state when scanning and requiring: $121~\mathrm{GeV} \leq m_{h_1}, m_{h_2} \leq 128~\mathrm{GeV}$ (Left) or $122~\mathrm{GeV} < m_{h_1} < 124~\mathrm{GeV}$, $125~\mathrm{GeV} < m_{h_2} < 127~\mathrm{GeV}$ (Right). Dashed lines show $m_h(ZZ) = m_h(\gamma\gamma) - (0, 0.5, 1, 1.5)$. **Hard to get a mass shift of more than $1~\mathrm{GeV}$.**

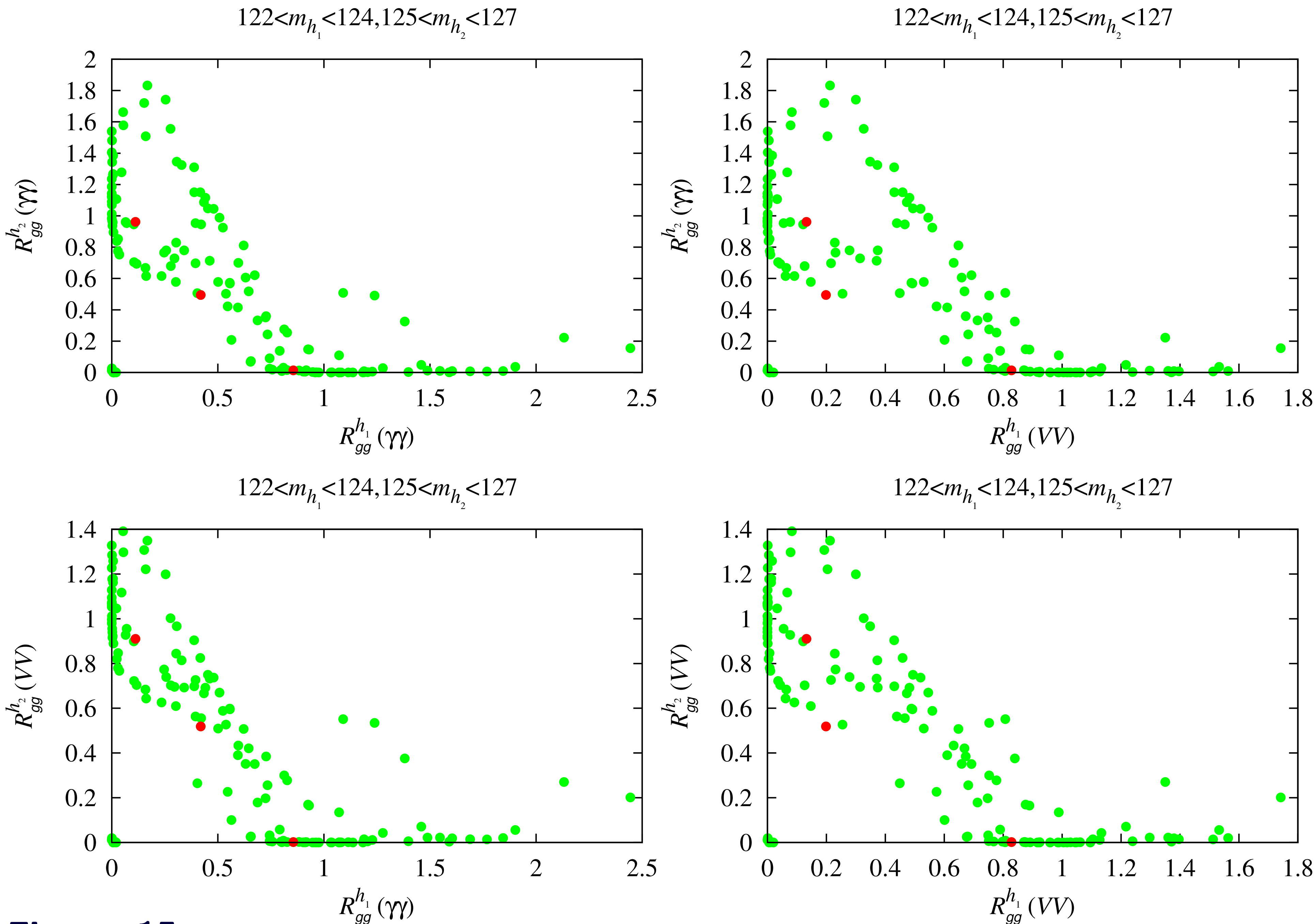

Figure 15: Too much correlation between VV and $\gamma\gamma$ channels for the h_1 and h_2 separately.

Diagnosing the presence of degenerate Higgses

(J. F. Gunion, Y. Jiang and S. Kraml. arXiv:1208.1817)

- Given that enhanced R^h_{gg} is very natural if there are degenerate Higgs mass eigenstates, how do we detect degeneracy if closely degenerate? Must look at correlations among different R^h's.
- In the context of any doublets plus singlets model not all the R^{h_i}'s are independent; a complete independent set of R^h's can be taken to be:

$$R^h_{gg}(VV), \quad R^h_{gg}(bb), \quad R^h_{gg}(\gamma\gamma), \quad R^h_{VBF}(VV), \quad R^h_{VBF}(bb), \quad R^h_{VBF}(\gamma\gamma)\,. \tag{9}$$

- Let us now look in more detail at a given $R^h_Y(X)$. It takes the form

$$R^h_Y(X) = \sum_{i=1,2} \frac{(C^{h_i}_Y)^2 (C^{h_i}_X)^2}{C^{h_i}_\Gamma} \tag{10}$$

where $C^{h_i}_X$ for $X = \gamma\gamma, WW, ZZ, \ldots$ is the ratio of the $h_i X$

to $h_{SM}X$ coupling and $C_\Gamma^{h_i}$ is the ratio of the total width of the h_i to the SM Higgs total width.

- The diagnostic tools that can reveal the existence of a second, quasi-degenerate (but non-interfering in the small width approximation) Higgs state are the double ratios:

$$\text{I}):\ \frac{R^h_{VBF}(\gamma\gamma)/R^h_{gg}(\gamma\gamma)}{R^h_{VBF}(bb)/R^h_{gg}(bb)},\quad \text{II}):\ \frac{R^h_{VBF}(\gamma\gamma)/R^h_{gg}(\gamma\gamma)}{R^h_{VBF}(VV)/R^h_{gg}(VV)},\quad \text{III}):\ \frac{R^h_{VBF}(VV)/R^h_{gg}(VV)}{R^h_{VBF}(bb)/R^h_{gg}(bb)},\quad (11)$$

each of which should be unity if only a single Higgs boson is present but, due to the non-factorizing nature of the sum in Eq. (10), are generally expected to deviate from 1 if two (or more) Higgs bosons are contributing to the net h signals.

- In a doublets+singlets model all other double ratios that are equal to unity for single Higgs exchange are not independent of the above three.
- Of course, the above three double ratios are not all independent. Which will be most useful depends upon the precision with

which the R^h's for different initial/final states can be measured. E.g measurements of R^h for the bb final state may continue to be somewhat imprecise and it is then double ratio II) that might prove most discriminating.

Or, it could be that one of the double ratios deviates from unity by a much larger amount than the others, in which case it might be most discriminating even if the R^h's involved are not measured with great precision.

- In Fig. 16, we plot the numerator versus the denominator of the double ratios I) and II), [III) being very like I) due to the correlation between the $R^h_{gg}(\gamma\gamma)$ and $R^h_{gg}(VV)$ values discussed earlier].
- We observe that any one of these double ratios will often, but not always, deviate from unity (the diagonal dashed line in the figure).
- The probability of such deviation increases dramatically if we

require (as apparently preferred by ATLAS data) $R^h_{gg}(\gamma\gamma) > 1$, see the solid (vs. open) symbols of Fig. 16.

- This is further elucidated in Fig. 17 where we display the double ratios I) and II) as functions of $R^h_{gg}(\gamma\gamma)$ (left plots).

  For the NMSSM, it seems that the double ratio I) provides the greatest discrimination between degenerate vs. non-degenerate scenarios with values very substantially different from unity (the dashed line) for the majority of the degenerate NMSSM scenarios explored in the earlier section of this talk that have enhanced $\gamma\gamma$ rates.

  Note in particular that I), being sensitive to the $b\bar{b}$ final state, singles out degenerate Higgs scenarios even when one or the other of h_1 or h_2 dominates the $gg \to \gamma\gamma$ rate, see the top right plot of Fig. 17.

  In comparison, double ratio II) is most useful for scenarios with $R^h_{gg}(\gamma\gamma) \sim 1$, as illustrated by the bottom left plot of Fig. 17.

- **Thus, as illustrated by the bottom right plot of Fig. 17, the greatest discriminating power is clearly obtained by measuring both double ratios.**

In fact, a close examination reveals that there are no points for which $both$ **double ratios are exactly 1!**

Of course, experimental errors may lead to a region containing a certain number of points in which both double ratios are merely consistent with 1 within the errors.

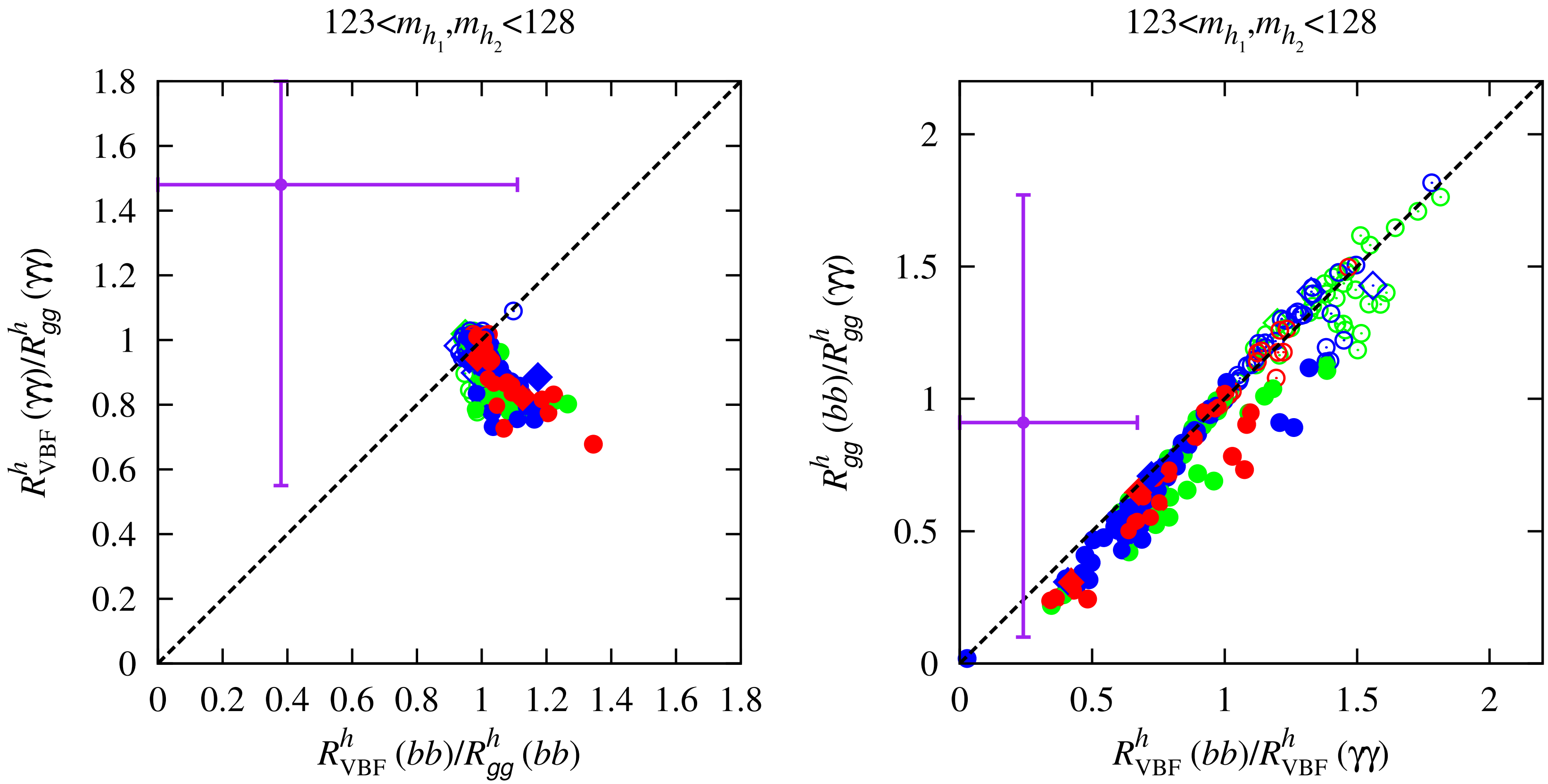

Figure 16: **Comparisons of pairs of event rate ratios that should be equal if only a single Higgs boson is present. The color code is green for points with $2~\mathrm{GeV} < m_{h_2} - m_{h_1} \leq 3~\mathrm{GeV}$, blue for $1~\mathrm{GeV} < m_{h_2} - m_{h_1} \leq 2~\mathrm{GeV}$, and red for $m_{h_2} - m_{h_1} \leq 1~\mathrm{GeV}$. Large diamond points have Ωh^2 in the WMAP window of $[0.094, 0.136]$, while circular points have $\Omega h^2 < 0.094$. Solid points are those with $R^h_{gg}(\gamma\gamma) > 1$ and open symbols have $R^h_{gg}(\gamma\gamma) \leq 1$. Current experimental values for the ratios from CMS data along with their 1σ error bars are also shown.**

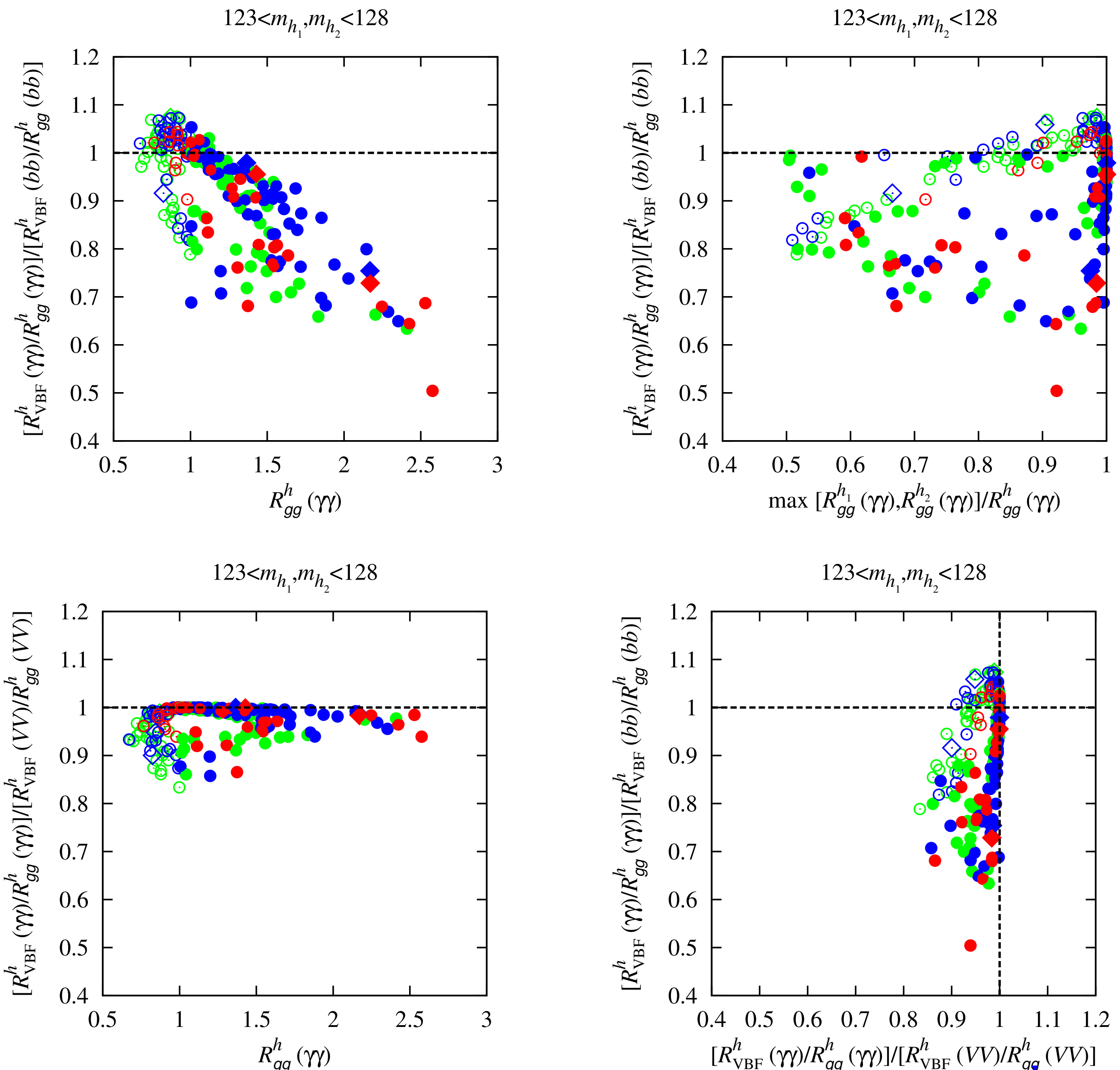

Figure 17: Double ratios I) and II) of Eq. (11) as functions of $R^h_{gg}(\gamma\gamma)$ (on the left). On the right we show (top) double ratio I) vs. $\max\left[R^{h_1}_{gg}(\gamma\gamma), R^{h_2}_{gg}(\gamma\gamma)\right]/R^h_{gg}(\gamma\gamma)$ and (bottom) double ratio I) vs. double ratio II) for the points displayed in Fig. 16. Colors and symbols are the same as in Fig. 16.

- **What does current LHC data say about these various double ratios?**

  The central values and 1σ error bars for the numerator and denominator of double ratios I) and II) obtained from CMS data (CMS-PAS-HIG-12-020) are also shown in Fig. 16.

  Obviously, current statistics are inadequate to discriminate whether or not the double ratios deviate from unity.

  About 100 times increased statistics will be needed. This will not be achieved until the $\sqrt{s} = 14~\mathrm{TeV}$ run with $\geq 100~\mathrm{fb}^{-1}$ of accumulated luminosity.

  Nonetheless, it is clear that the double-ratio diagnostic tools will ultimately prove viable and perhaps crucial for determining if the $\sim 125~\mathrm{GeV}$ Higgs signal is really only due to a single Higgs-like resonance or if two resonances are contributing.

- **Degeneracy has significant probability in model contexts if enhanced $\gamma\gamma$ rates are indeed confirmed at higher statistics.**

Higgs-radion mixing model example

– **Much bigger deviations of double ratios from being equal, related to anomalous gg and $\gamma\gamma$ couplings of the radion. (Compare to first NMSSM plot of preceding section)**

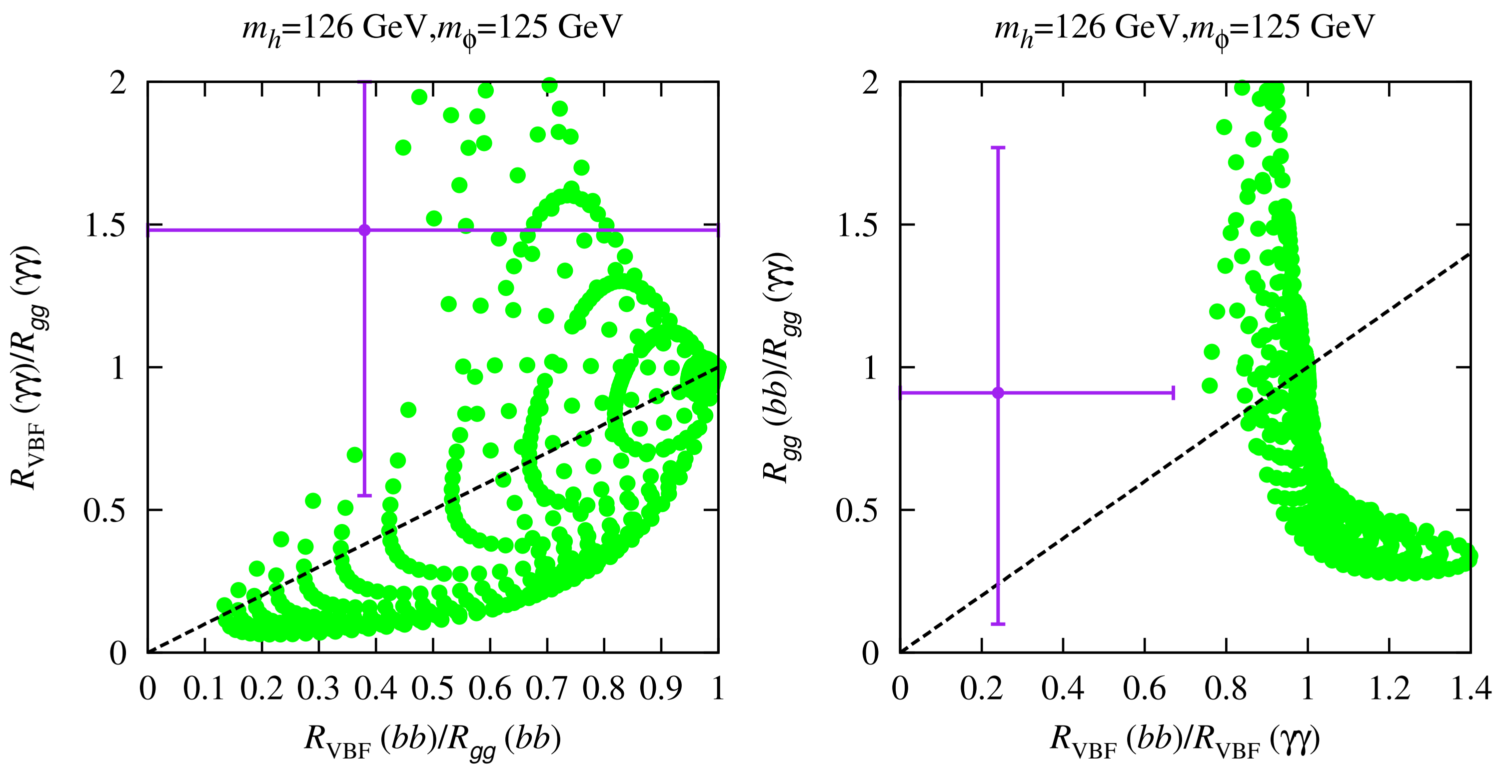

Figure 18: **Figure shows only a small part of the full range of vertical axis.**

The pure 2HDM

- *"Two-Higgs-Doublet Models and Enhanced Rates for a 125 GeV Higgs"* **A. Drozd, B. Grzadkowski, J. F. Gunion and Y. Jiang. arXiv:1211.3580 [hep-ph]**
- **see also,** *"Mass-degenerate Higgs bosons at 125 GeV in the Two-Higgs-Doublet Model"* **P. M. Ferreira, H. E. Haber, R. Santos and J. P. Silva. arXiv:1211.3131 [hep-ph]**
- **There are some differences.**

NMSSM-like degeneracy can be explored in this context also, but no time to discuss.

Conclusions

- It seems likely that the Higgs responsible for EWSB has emerged.
- Perhaps, other Higgs-like objects are emerging.
- Survival of enhanced signals for one or more Higgs boson would be one of the most exciting outcomes of the current LHC run and would guarantee years of theoretical and experimental exploration of BSM models with elementary scalars.
- $>$SM signals would appear to guarantee the importance of a linear collider or LEP3 or muon collider in order to understand fully the responsible BSM physics.
- In any case, the current situation illusrates the fact that we must never assume we have uncovered all the Higgs.

Certainly, I will continue watching and waiting